# $\frac{3}{2}^+$ levels of $^5$He and $^5$Li, and shadow poles

F. C. Barker
*Department of Theoretical Physics, Research School of Physical Sciences and Engineering, The Australian National University, Canberra ACT 0200, Australia*
(Received 19 February 1997)

It is suggested that, contrary to previous proposals, the properties of the $\frac{3}{2}^+$ levels of $^5$He and $^5$Li may be understood as easily from the conventional $R$-matrix parameters as from the complex-energy poles of the $S$ matrix. [S0556-2813(97)02211-5]

PACS number(s): 24.30.−v, 25.10.+s, 27.10.+h

## I. INTRODUCTION

The most recent compilation for $A=5$ nuclei [1] gives the lowest $\frac{3}{2}^+$ level of $^5$He at an excitation energy of 16.75 MeV, about 50 keV above the $^3$H+$d$ threshold, with a width of 76 keV shared almost equally between the $^3$H+$d$ and $^4$He+$n$ channels. As well as being of importance in the production of thermonuclear energy, this level has several interesting properties, which are exhibited in the $^3$H$(d,n)^4$He reaction cross section, the $^4$He+$n$ total cross section, and the $^3$H+$d$ and $^4$He+$n$ elastic scattering phase shifts.

Comprehensive multilevel, multichannel $R$-matrix fits have been made to the data [2]. The data for $E_d \lesssim 250$ keV have also been fitted using a one-level, two-channel approximation [3]. Fits to more recent and more extensive data have used two- and four-level approximations [2,4].

Hale [5] has pointed out that it is not always easy to interpret multilevel $R$-matrix parameters, and that it would be better to extract resonance properties from an asymptotic quantity such as the $S$ matrix. Pearce and Gibson [6] say ''it is not possible to determine from the $R$-matrix parametrization . . . whether it is the $n\alpha$ or $dt$ channel that is responsible for the $J^\pi=\frac{3}{2}^+$ resonance in $^5$He.'' Recently, Csoto and Hale [7], in a paper on the low-lying levels of $^5$He and $^5$Li, conclude ''we recommend using the complex $S$-pole prescription to specify resonance parameters in all cases,'' and they say, with particular reference to the $\frac{3}{2}^+$ level of $^5$He, ''Only analyses at complex energies were able to reveal that the large reaction cross section [for $^3$H$(d,n)^4$He] is caused by a shadow pole of the scattering matrix.''

For each of the one-, two-, and four-level $R$-matrix fits, two complex-energy poles of the corresponding $S$ matrix have been found [4], with real parts about 48 keV and 80 keV, lying on different (unphysical) sheets of the two-channel Riemann energy surface. The 48 keV pole is of conventional type, while the 80 keV pole has been identified [4,8] as a shadow pole [9]. Here, we consider the alternative interpretations of various properties of the $\frac{3}{2}^+$ level of $^5$He (and of its analog level in $^5$Li) in terms of either the complex-energy poles of the $S$ matrix or the conventional $R$-matrix parameters.

Among the properties that need explanation are (1) the nature of the $\frac{3}{2}^+$ resonance; (2) the very large value (nearly the maximum possible) of the $^3$H$(d,n)^4$He cross section $\sigma_{dn}$ at the resonance [10]; (3) the energies and full widths at half maximum (FWHM) of the measured peaks in $\sigma_{dn}$ [3] and the $^4$He+$n$ total cross section $\sigma_T$ [11]; (4) the difference in the character of the $^4$He+$n$ $d_{3/2}$ phase shift as measured [12] and as predicted [13] from models that fit other data; and (5) the different characters of the predicted $^3$H+$d$ $s$-wave phase shift [13] and the measured $^3$He+$d$ $s$-wave phase shift [14].

## II. ALTERNATIVE INTERPRETATIONS

The formulas connecting cross sections and phase shifts with the elements of the $S$ matrix, which are common to both interpretations, are taken from Lane and Thomas [15] (where the $S$ matrix is denoted by $U$).

The integrated cross section $\sigma_{dn}$ for the $^3$H$(d,n)^4$He reaction, with $d$ labeling the $^3$H+$d$ $s$-wave channel and $n$ the $^4$He+$n$ $d$-wave channel, is given by

$$\sigma_{dn}=\frac{\pi}{k_d^2}\frac{2}{3}|S_{dn}|^2, \tag{1}$$

where $k_d$ is the deuteron wave number in the c.m. system. The corresponding astrophysical $S$ factor is defined by

$$S=Ee^{2\pi\eta}\sigma_{dn}, \tag{2}$$

where $E$ is the c.m. energy in the $^3$H+$d$ system and $\eta$ is the Sommerfeld parameter.

The phase shifts $\delta_c$ $(c=d,n)$ are defined by

$$S_{cc}=e^{2i(\omega_c+\delta_c)}=\tau e^{2i(\omega_c+\mu_c)}, \tag{3}$$

where $\omega_c$ is the Coulomb phase shift (in the present case, $\omega_d=0$ because $l_d=0$, and $\omega_n=0$ because the neutron is uncharged), $\mu_c=\mathrm{Re}\,\delta_c$ and the inelastic parameter $\tau=e^{-2\,\mathrm{Im}\,\delta_c}=[1-|S_{dn}|^2]^{1/2}$. The corresponding scattering amplitude is [12]

$$f_c=\frac{e^{2i\delta_c}-1}{2i}. \tag{4}$$

The total $^4$He+$n$ cross section is

 

$$\sigma_T=\frac{\pi}{k_n^2}4[1-\mathrm{Re}(e^{-2i\omega_n}S_{nn})]=\frac{4\pi}{k_n^2}[1-\tau\cos 2\mu_n]. \tag{5}$$

### A. Complex-energy poles of the *S* matrix

We consider how the properties listed in Sec. I have been interpreted [8,13] in terms of the $S$-matrix poles, which are located at the complex energies $E_r-i\Gamma/2$. As in Refs. [8, 13], we use the values of the $S$-matrix pole parameters given by Hale *et al.* [8] for the four-level $R$-matrix fit. The conventional pole is at $E_r=47.0$ keV with a width $\Gamma=74.2$ keV, while the shadow pole has $E_r=81.6$ keV and $\Gamma=7.3$ keV. Here and elsewhere, energies and widths are in the $^3$H$+d$ c.m. system, unless otherwise specified. Hale *et al.* also give values of the partial widths for the $s$-wave deuteron and $d$-wave neutron channels; the $d$-wave deuteron partial widths are negligible. Qualitatively similar $S$-matrix parameter values come from the one-level, two-channel fit of Jarmie *et al.* [3] and from the two-level, two-channel fit of Brown *et al.* [4] (see Table IV in Ref. [4]).

(1) From the sheet on which the shadow pole lies, Hale *et al.* [8] concluded that the $\frac{3}{2}^+$ resonance in $^5$He originates from the $^4$He$+n$ channel. Later work [6,13,16] showed that the shadow pole can move from one sheet to another as the coupling between the $^3$H$+d$ and $^4$He$+n$ channels changes, and that the sheet on which the shadow pole lies in the limit of zero coupling identifies the resonance as associated with the $^3$H$+d$ channel.

(2) Hale *et al.* [8] show their calculated $|S_{dn}|^2$ peaking at $E\approx 82$ keV, and so they attribute the peak in $\sigma_{dn}$ to the shadow pole. The shadow pole (on an unphysical sheet) is associated with a zero of $S_{nn}$ on the physical sheet at the same complex energy. The smallness of $\Gamma$ for the shadow pole means that $|S_{nn}|$ becomes very small for real energies near $E_r$, and unitarity then forces $|S_{dn}|$ to approach its maximum value of unity [8]. The smallness of $\Gamma$ for the shadow pole is related to the smallness [12] of the inelastic parameter $\tau$ at resonance [6]. The connection, if any, between this value of $\Gamma$ (7.3 keV) and the FWHM of $\sigma_{dn}$ (about 80 keV from Fig. 11 of Ref. [3]) is not explained in Ref. [8].

(3) Although the calculated $|S_{dn}|^2$ peaks at about 82 keV, $\sigma_{dn}$ and $S$ given by Eqs. (1) and (2) peak at much lower energies, about 64 keV and 49 keV, respectively, in good agreement with the experimental values [3]. Hale *et al.* [8] calculate the peak of $(1-\mathrm{Re}\,S_{nn})$, and therefore of $\sigma_T$, at about 58 keV. They therefore say that the conventional pole at $E_r=47.0$ keV is mainly responsible for the peak in $\sigma_T$. They obtain good agreement with the $\sigma_T$ measurement of Haesner *et al.* [11], who found the peak at $E_n$(lab) $=22133\pm 10$ keV, corresponding to $E=54\pm 8$ keV.[1] There is also good agreement between $\Gamma=74.2$ keV for the conventional pole [8] and the measured FWHM of the $\sigma_T$ peak of $76\pm 12$ keV [11], and between the partial width $\Gamma_n$ $=39.8$ keV for the conventional pole [8] and Haesner *et al.*'s value of $37\pm 5$ keV [11].

The approximate equality of the energies of the $\sigma_{dn}$ and $\sigma_T$ peaks (about 64 keV and $54\pm 8$ keV, respectively) and of their FWHM (about 80 keV and $76\pm 12$ keV) is somewhat surprising if the peak in $\sigma_{dn}$ is attributed to the shadow pole and the peak in $\sigma_T$ to the conventional pole, as in Ref. [8].

(4) Hoop and Barschall [12] made a phase-shift analysis of their $^4$He$+n$ elastic scattering measurements. They found that, as the energy increases through the $\frac{3}{2}^+$ resonance, the real part $\mu_n$ of the $d_{3/2}$ phase shift first increases, then decreases rapidly at the resonance energy by about 70°, and finally increases slowly to near its initial value. Simultaneously the inelastic parameter $\tau$ decreases from unity to a small value at the resonance, then increases.

Csoto *et al.* [13] calculated the $^4$He$+n$ $d_{3/2}$ phase shift from a resonating-group type microscopic model with potential adjusted to fit predictions of the four-level $R$-matrix fit [8] for the $^3$H$+d$ $s$-wave phase shift and for $|S_{dn}|^2$. The calculated $\mu_n$ increases rapidly at the resonance, rather than decreasing. By slightly reducing the coupling strength, the calculated $\mu_n$ could be made similar to that measured [12], but at the expense of spoiling the agreement with the $^3$H$+d$ phase shift [13]. In terms of the $S$-matrix poles, the reduced coupling strength moves the shadow pole onto a different sheet of the Riemann surface, which has the effect of changing the characters of both the $^4$He$+n$ and $^3$H$+d$ phase shifts [6,13].

It may be noted that Hoop and Barschall [12] said that, although their data are fitted best with a phase shift that decreases rapidly at the resonance, the possibility of a rapid increase could not be excluded.

(5) The $A=5$ compilation [1] gives the analogous $\frac{3}{2}^+$ level of $^5$Li at about 270 keV above the $^3$He$+d$ threshold, with a width of about 200 keV. Analysis of the $^3$He$+d$ elastic scattering data gives the $s$-wave phase shift with the real part increasing smoothly through the $\frac{3}{2}^+$ resonance [14].

The $^3$H$+d$ elastic scattering differential cross section in the resonance region has been measured only at 90° [17], which is not enough for a complete phase-shift analysis. Bogdanova *et al.* [16] show that the $s$-wave phase shift, calculated from a model with parameter values adjusted to best fit the $^3$H$+d$ scattering amplitude predicted by the four-level $R$-matrix fit [8], gives a 90° differential cross section consistent with that measured [17]. The phase shift $\mu_d$ from the four-level fit is shown in Fig. 1 of Csoto *et al.* [13]; it decreases as the energy increases through the resonance.

The different character of the $^3$He$+d$ and $^3$H$+d$ $s$-wave phase shifts is attributed [13] to the shadow poles in the two cases being on different sheets, due to the different charges involved.

We note that the $^3$H$+d$ $s$-wave phase shift extracted by Balashko [17] from his data, using plausible assumptions about the other phase shifts, increases smoothly with increasing energy, contrary to the prediction from the four-level $R$-matrix fit [8].

### B. *R*-matrix parameters

General multilevel, multichannel formulas for the elements of the scattering matrix in terms of $R$-matrix parameters are given by Lane and Thomas [15]:

[1]I am indebted to Hale for pointing out the need to use relativistic kinematics for 22 MeV neutrons.

$$S_{cc'}=\Omega_c\Omega_{c'}\left[\delta_{cc'}+2iP_c^{1/2}P_{c'}^{1/2}\sum_{\lambda\mu}\gamma_{\lambda c}\gamma_{\mu c'}A_{\lambda\mu}\right], \qquad (6)$$

where

$$\Omega_c=e^{i(\omega_c-\phi_c)} \qquad (7)$$

and the level matrix **A** is defined by its inverse

$$(\mathbf{A}^{-1})_{\lambda\mu}=(E_\lambda-E)\delta_{\lambda\mu}-\sum_c(S_c-B_c+iP_c)\gamma_{\lambda c}\gamma_{\mu c}. \qquad (8)$$

Here $S_c$, $P_c$, and $-\phi_c$, which are the energy-dependent shift factor, penetration factor, and hard-sphere phase shift for the channel $c$, are known functions of the channel radius $a_c$, and $B_c$ is the constant boundary condition parameter, while $E_\lambda$ and $\gamma_{\lambda c}$ are the eigenenergy and reduced width amplitude for the level $\lambda$.

In order to understand the properties of the $\frac{3}{2}^+$ level of $^5$He, it is simplest to consider a one-level, two-channel fit to the data. Such fits were made to quite different data by Jarmie *et al.* [3] and by Hoop and Barschall [12]; both give values of their $R$-matrix parameters $a_c$, $B_c$, $E_\lambda$, and $\gamma_{\lambda c}$. Hale *et al.* [8] give the $R$-matrix parameter values for their four-level, four-channel fit. They say that the lowest of the four levels is primarily responsible (>99%) for the two $S$-matrix poles discussed in Sec. II A, so that for the present purposes it would seem to be reasonable to approximate their fit by retaining only this level. We also omit the two $d$-wave deuteron channels, which contribute little at low energies.

In this one-level, two-channel ($c=d,n$) approximation, one has

$$S_{dd}=e^{-2i\phi_d}\left[1+\frac{i\Gamma_d}{E_1+\Delta-E-(1/2)i\Gamma}\right], \qquad (9)$$

$$|S_{dn}|^2=\frac{\Gamma_d\Gamma_n}{(E_1+\Delta-E)^2+[(1/2)\Gamma]^2}, \qquad (10)$$

and

$$S_{nn}=e^{-2i\phi_n}\left[1+\frac{i\Gamma_n}{E_1+\Delta-E-(1/2)i\Gamma}\right], \qquad (11)$$

where

$$\Gamma=\sum_c\Gamma_c, \quad \Gamma_c=2\gamma_c^2P_c,$$

$$\Delta=\sum_c\Delta_c, \quad \Delta_c=-\gamma_c^2[S_c-B_c]. \qquad (12)$$

It should be noted that $\Gamma$ and $\Delta$ are energy dependent. The resonance energy $E_r$ is defined by

$$E_1+\Delta(E_r)-E_r=0. \qquad (13)$$

The quantities $E_r$ and $\Gamma$ here are not necessarily the same as the $E_r$ and $\Gamma$ in Sec. II A. In order to discuss the widths, it is useful to introduce the Thomas approximation [18]. This is based on the assumption that the shift factors $S_c$ are linear functions of energy over the resonance region. In this approximation, "observed" partial widths are defined by

$$\Gamma_c^0=\Gamma_c/(1-d\Delta/dE)_{E_r}$$
$$=2\gamma_c^2P_c\Big/\left(1+\sum_c\gamma_c^2dS_c/dE\right)_{E_r}. \qquad (14)$$

Then

$$S_{dd}=e^{-2i\phi_d}\left[1+\frac{i\Gamma_d^0}{E_r-E-(1/2)i\Gamma^0}\right] \quad (\Gamma^0=\Gamma_d^0+\Gamma_n^0), \qquad (15)$$

$$|S_{dn}|^2=\frac{\Gamma_d^0\Gamma_n^0}{(E_r-E)^2+[(1/2)\Gamma^0]^2}, \qquad (16)$$

$$S_{nn}=e^{-2i\phi_n}\left[1+\frac{i\Gamma_n^0}{E_r-E-(1/2)i\Gamma^0}\right]. \qquad (17)$$

It is $\Gamma^0$ rather than $\Gamma$ that in general approximates the FWHM of a peak.

We now consider how the properties listed in Sec. I are to be understood in terms of the $R$-matrix parameters, together with the penetration factors, shift factors, and hard-sphere phase shifts, all calculated at real energies only. Some of these considerations resemble those in the literature around 40 years ago.

(1) The reduced width $\gamma_c^2$ is related to the spectroscopic factor $\mathcal{S}_c$ by [15,19]

$$\gamma_c^2=(\hbar^2/M_ca_c^2)\mathcal{S}_c\theta_{sp}^2(c), \qquad (18)$$

where $M_c$ is the reduced mass, and the single-particle dimensionless reduced width is defined by

$$\theta_{sp}^2(c)=(a_c/2)u_c^2(a_c)\Big/\int_0^{a_c}u_c^2(r)dr. \qquad (19)$$

Here $r^{-1}u_c(r)$ is the radial wave function in channel $c$; we calculate it for a central Woods-Saxon potential with conventional radius and diffuseness parameters, cut off at $r=a_c$, and with the depth adjusted to fit the energy of the resonance in the channel. For the one-level approximation to the Hale *et al.* fit [8], one finds $\theta_{sp}^2(d)=0.88$ and $\theta_{sp}^2(n)=1.17$, giving $\mathcal{S}_d=1.18$ and $\mathcal{S}_n=0.021$, with $\mathcal{S}_d/\mathcal{S}_n\approx 56$. This ratio is not sensitive to the potential parameters. Similarly large values are found for the one-level fits [3,12] (see also Table 5.2 in Ref. [20]). The large value of $\mathcal{S}_d/\mathcal{S}_n$ makes it natural to associate the resonance with the deuteron channel rather than the neutron channel. In addition, one can investigate the reasons why $\mathcal{S}_d$ and $\mathcal{S}_n$ are so different, and why the $\frac{3}{2}^+$ resonance is so close to the $^3$H$+d$ threshold. In a shell model calculation [21], using an interaction chosen to fit properties of other light nuclei, the lowest $\frac{3}{2}^+$ state of $^5$He at an excitation energy of 14.5 MeV is mainly of $^4$He$+n$ structure; its calculated width is therefore so large that it would not appear as an experimentally identifiable peak. The observed $\frac{3}{2}^+$ level is identified with the

TABLE I. Parameter values for one-level $R$-matrix fit to $\sigma_{dn}$ and $\sigma_T$ data. The background phase shift in the neutron channel is taken as $\phi=-3.29°+0.510°E_n(\mathrm{lab})$, with $E_n(\mathrm{lab})$ in MeV, and the background contribution to $\sigma_T$ is $A+BE_n(\mathrm{lab})$.

| $a_d$ (fm) | $a_n$ (fm) | $B_d$ | $B_n$ | $E_1$ (MeV) | $\gamma_d^2$ (MeV) | $\gamma_n^2$ (MeV) | A ($b$) | B ($b$ MeV$^{-1}$) |
|---|---|---|---|---|---|---|---|---|
| 6.0 | 5.0 | −0.285 | −0.197 | 0.0912 | 2.93 | 0.0794 | 1.050 | −0.0160 |

second $\frac{3}{2}^+$ shell model state, which is mainly of $^3$H$+d$ structure and therefore has a large value of $\mathcal{S}_d$, while $\mathcal{S}_n$ is calculated to be 0.005 [21].

An enhanced probability of finding a level close to the threshold of a channel for which it has a large spectroscopic factor has been derived [22] from $R$-matrix formulas; for the present case, the enhancement factor for the $\frac{3}{2}^+$ level of $^5$He being close to the $^3$H$+d$ threshold is calculated to be about six [22].

(2) The cross section $\sigma_{dn}$ is given in terms of $|S_{dn}|^2$ in Eq. (1). From Eqs. (10) and (13), at $E=E_r$, one has $|S_{dn}|^2=4\Gamma_d\Gamma_n/(\Gamma_d+\Gamma_n)^2$, which has its maximum value of unity when $\Gamma_d=\Gamma_n$. In the four-level fit of Hale *et al.* [8], $|S_{dn}|^2$ peaks at $E\approx 82$ keV, and at this energy their parameter values for the lowest $R$-matrix level give $\Gamma_d=260$ keV and $\Gamma_n=409$ keV, with $4\Gamma_d\Gamma_n/(\Gamma_d+\Gamma_n)^2=0.95$. For the one-level fits of Refs. [3,12], this quantity is 0.98 and 0.999, respectively. Thus the large value of $\sigma_{dn}$ at resonance is attributed to the near equality of $\Gamma_d$ and $\Gamma_n$ at the resonance (cf., e.g., Ref. [10]).

(3) The measured peak energy of $\sigma_{dn}$ is about 64 keV [3], while Haesner *et al.* [11] give the $\sigma_T$ peak at $54\pm 8$ keV. The corresponding FWHM are about 80 keV [3] and $76\pm 12$ keV [11], respectively.

The four-level fit of Hale *et al.* [8] and the one-level fits of Jarmie *et al.* [3] and Hoop and Barschall [12] each included measured $\sigma_{dn}$ values in their fits, and so reproduce the energy of the $\sigma_{dn}$ peak reasonably well. Hale *et al.* and Hoop and Barschall give similar predictions for $\sigma_T$ with the peak energy at about 58 keV, in good agreement with the measured value [11]. Jarmie *et al.* predict the peak energy at about 95 keV, and their peak is much too broad.

From Eq. (5), together with Eq. (11) or (17), it is seen that $\sigma_T$ may depend sensitively on the value of $\phi_n$. In this one-level approximation, the $d_{3/2}$ neutron background phase shift (which we call $\phi$ as in [12]), is just $-\phi_n$, the hard-sphere phase shift. Jarmie *et al.* used a channel radius $a_n=3$ fm for which $\phi_n\approx 29°$. Hoop and Barschall took $a_n=5$ fm, for which $\phi_n\approx 98°$, but in order to fit their data they used $\phi=5°$. Hale *et al.* also used $a_n=3$ fm, $\phi_n\approx 29°$, but contributions from the three higher levels could change the effective value of $\phi$.

The background phase shift has actually been measured for $E_n(\mathrm{lab})$ up to 20 MeV [23], and extrapolation to the resonance energy gives $\phi\approx 8°$. If one takes as an approximation $\phi_n=0$ in Eq. (17), then one obtains

$$\sigma_T=\frac{2\pi}{k_n^2}\frac{(\Gamma_d^0+\Gamma_n^0)\Gamma_n^0}{(E_r-E)^2+[(1/2)\Gamma^0]^2}. \quad (20)$$

Comparison with Eq. (16) for $|S_{dn}|^2$ suggests that, since $k_n^2$ and $\Gamma_n^0$ are slowly varying functions of $E$, $\sigma_T$ should peak at a higher energy than the $S$ factor for $^3$H$(d,n)^4$He but at a lower energy than $|S_{dn}|^2$, i.e., between 49 keV and 82 keV.

One cannot obtain $\phi=8°$ as a hard-sphere phase shift, but the equivalent value $\phi=8°-180°=-172°$ is the value of $-\phi_n$ for $a_n\approx 7$ fm. The use of a ''small'' channel radius, $a_n=3$ fm, in Refs. [3,4,8] presumably originated in the work of Adair [24] and Dodder and Gammel [25], who chose $a=2.9$ fm in order to fit the low-energy $p_{1/2}$ and $p_{3/2}$ $^4$He$+$nucleon phase shifts with one-level approximations and to account for the Coulomb energy difference between $^5$Li and $^5$He. More recently, consistent $R$-matrix analyses of these phase shifts and of data from reactions in which $^5$He and $^5$Li are product nuclei, using two-level approximations, have led to a best channel radius of $5.5\pm 1.0$ fm [26]. A two-level fit of the $d_{3/2}$ phase-shift data for $E_n(\mathrm{lab})\leqslant 20$ MeV [23] gives the energy of the lowest $\frac{3}{2}^+$ level at about 14 MeV for $a_n=5.1$ fm, in agreement with the shell model value.

One could try to fit the data in the neighborhood of the 16.75 MeV $\frac{3}{2}^+$ level of $^5$He with a three-level $R$-matrix approximation, one of the levels being the 16.75 MeV resonance itself and the other two providing the background phase shift in the neutron channel. It is simpler, however, and probably adequate, to use the one-level approximation, but with the background phase $\phi$ in the neutron channel adjusted to fit the measured values [23]. We use a quadratic extrapolation to obtain $\phi$ in the resonance region. In this way we have attempted to fit the $\sigma_{dn}$ [3,4,27] and $\sigma_T$ (Fig. 4 of Ref. [11]) data. A linear function of energy is included to represent the background contribution to $\sigma_T$ (see Fig. 3 of Ref. [11]).

For given values of the channel radii $a_d$ and $a_n$, and with $B_d$ and $B_n$ chosen to make $S_c(E_r)=B_c$, there are then five adjustable parameters: $E_1,\gamma_d^2,\gamma_n^2$, and the two parameters in the linear background. For $a_d=6.0$ fm and $a_n=5.0$ fm, the parameter values that best fit the $\sigma_{dn}$ and $\sigma_T$ data, with $\chi^2$/degree of freedom $\approx 1.0$, are given in Table I. The corresponding fits are shown in Figs. 1 and 2. Allowance for the experimental resolution of about 30 keV FWHM in the $\sigma_T$ data [11] has little effect on either $\chi^2$ or the parameter values. There is little dependence on the value of $a_n$ (as long as $\phi$ is not changed). A slightly better fit is obtained with $a_d=5.0$ fm, but for a much larger value of $\gamma_d^2$, implying a value of $\mathcal{S}_d$ much greater than unity. This is connected with the upper limit on $\Gamma_d^0$, obtained as $\gamma_d^2\to\infty$ in Eq. (14), becoming smaller as $a_d$ becomes smaller.

A slightly better fit is also obtained if the background phase $\phi$ is increased by about 30%, but such an increase appears to be inconsistent with the experimental values of $\phi$ at lower energies [23].

From Fig. 2, the peak of the $d_{3/2}$ contribution to $\sigma_T$ is at $E_n(\mathrm{lab})=22.139$ keV, corresponding to $E=59$ keV, and its FWHM is about 138 keV (lab) or 110 keV (c.m.). These

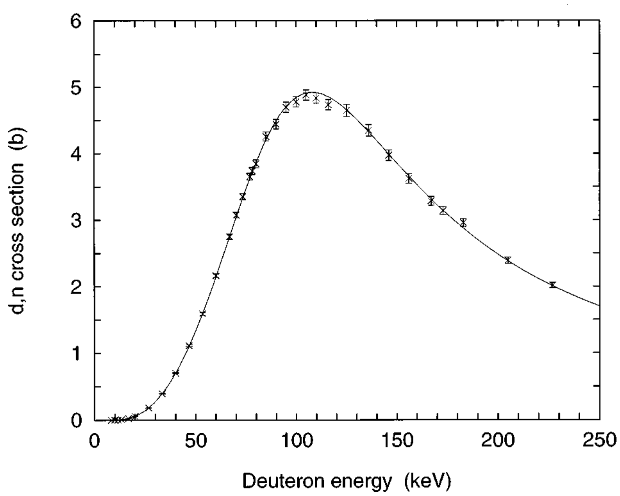


FIG. 1. Cross section $\sigma_{dn}$ for the $^3$H$(d,n)^4$He reaction as a function of deuteron lab energy $E_d$. The experimental data are from Jarmie *et al.* [3] ($E_d=8-78$ keV), Brown *et al.* [4] ($E_d=80-116$ keV), and Conner *et al.* [27] ($E_d=125-227$ keV, with $\sigma_{dn}$ assumed isotropic and normalized at peak to Ref. [4]). The calculated curve is for the one-level fit with parameter values given in Table I.

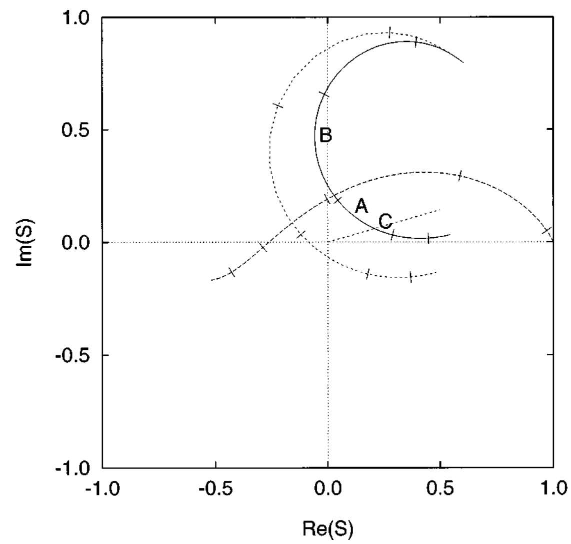


FIG. 3. Argand diagram for $S$-matrix elements: $S_{nn}$ for one-level fit (solid curve); $S_{dd}$ for one-level fit (dashed curve); $S_{nn}$ for four-level fit of Hale *et al.* [8] (dotted curve). On each curve, the marks indicate values of $E$ increasing (in an anticlockwise sense) from 25 to 125 keV, in 25 keV steps. The dotted straight line has a slope of $2\phi(E_r)\approx 16°$. The points $A$, $B$, and $C$ indicate the energy at which $|S_{dn}|^2$ is a maximum, the energy at which $\sigma_T$ is a maximum, and the resonance energy $E_r$, respectively.

agree well with the predictions from the four-level fit of Hale *et al.* [8] of $E\approx 58$ keV and FWHM$\approx$105 keV. The FWHM is appreciably greater than the value $76\pm 12$ keV given by Haesner *et al.* [11], presumably because they assumed a Breit-Wigner shape for the peak, resulting in a significantly higher background. A similar comment applies to the earlier measurement of $\sigma_T$ by Shamu and Jenkin [28], who found a FWHM of 105 keV (lab) or 84 keV (c.m.) (not $100\pm 50$ keV as stated in Ref. [11]). Shamu and Jenkin gave the peak energy as $E_n$(lab)$=22.15$ MeV; since they used neutrons produced in the $^3$H$(d,n)^4$He reaction, for which they took the $Q$ value as 22.07 MeV, their peak was about 80 keV (lab) above threshold, corresponding to $E\approx 64$ keV.

The relationship between the resonance energy $E_r=E_1=91$ keV and the peak energies for $|S_{dn}|^2$ and $\sigma_T$ is made clear by plotting $S_{nn}$ on an Argand diagram, as in Fig. 3 (a plot of the scattering amplitude $f_n$ gives similar information). Since $|S_{dn}|^2+|S_{nn}|^2=1$ from unitarity, $|S_{dn}|^2$ is a maximum when $|S_{nn}|^2$ is a minimum, at the point marked $A$ ($E_a=77$ keV). Because $E_n$ varies little over the resonance, $\sigma_T$ is a maximum where Re($S_{nn}$) is a minimum, at the point $B$ ($E_b=58$ keV). At the resonance energy $E_r$ (point $C$), the argument of $S_{nn}$ is $2\phi(E_r)\approx 16°$ [see Eq. (17)]. This fit gives $E_b<E_a$. The one-level fit of Jarmie *et al.* [3] gives $E_b>E_a$, due to their background neutron phase shift $\phi$ being about $-29°$ (which is inconsistent with the measurements of Ref. [23]). The plot of $S_{nn}$ for their fit is obtained from that of the one-level fit in Fig. 3 essentially by rotation about the origin in a clockwise direction by $2(8°+29°)=74°$; then Re($S_{nn}$) increases very slowly for energies above $E_b$, giving a very long tail to $\sigma_T$.

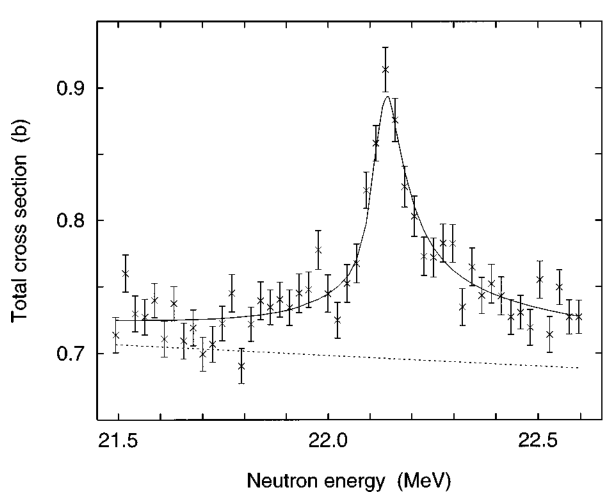


FIG. 2. $^4$He$+n$ total cross section $\sigma_T$ as a function of neutron lab energy $E_n$. The experimental data are from Haesner *et al.* [11]. The solid curve shows the calculated one-level fit with parameter values given in Table I. The dotted curve shows the background.

Figure 3 also shows $S_{nn}$ for the four-level fit of Hale *et al.* [8]. It is seen that, compared with the one-level fit, the four-level fit gives the $\sigma_{dn}$ peak 2.3% higher and the $d_{3/2}$ contribution to the $\sigma_T$ peak 19% higher. From Fig. 2, it might seem that a higher $\sigma_T$ peak would be desirable; we have, however, been unable to obtain a good fit to all the data with an appreciably larger value of $\gamma_n^2/\gamma_d^2$.

The values of the various widths, calculated for the one-level fit at the energy $E_a=77$ keV, are $\Gamma_d=645$ keV, $\Gamma_n=543$ keV, $\Gamma_d^0=92$ keV, $\Gamma_n^0=77$ keV, $\Gamma^0=169$ keV. This value of $\Gamma^0$ is somewhat smaller than the FWHM of the $|S_{dn}|^2$ peak (about 210 keV), but the FWHM of $\sigma_{dn}$ is much smaller (about 80 keV) due to the factor $k_d^{-2}$ in Eq. (1).

(4) From Eqs. (3), (15), and (17), the inelastic parameter is given by

$$\tau=\left[\frac{(E_r-E)^2+(1/4)(\Gamma_d^0-\Gamma_n^0)^2}{(E_r-E)^2+(1/4)(\Gamma_d^0+\Gamma_n^0)^2}\right]^{1/2}, \qquad (21)$$

and the real parts of the phase shifts by

$$\mu_d=\frac{1}{2}\arctan\frac{(1/2)(\Gamma_d^0+\Gamma_n^0)}{E_r-E}+\frac{1}{2}\arctan\frac{(1/2)(\Gamma_d^0-\Gamma_n^0)}{E_r-E}-\phi_d,$$

$$\mu_n=\frac{1}{2}\arctan\frac{(1/2)(\Gamma_d^0+\Gamma_n^0)}{E_r-E}-\frac{1}{2}\arctan\frac{(1/2)(\Gamma_d^0-\Gamma_n^0)}{E_r-E}-\phi_n. \quad (22)$$

For a one-channel case, the phase shift is real and is given by [15]

$$\delta=\arctan\frac{(1/2)\Gamma^0}{E_r-E}-\phi; \quad (23)$$

$\delta$ increases by about 90° over the energy interval $\Gamma^0$ around $E_r$. Thus from Eq. (22), $\mu_d$ increases by about 45° over a width $\Gamma^0=\Gamma_d^0+\Gamma_n^0$, with an additional change by about 45° over a width of $|\Gamma_d^0-\Gamma_n^0|$, this being an increase or a decrease according to whether $\Gamma_d^0$ is greater than or less than $\Gamma_n^0$ at $E=E_r$. This change becomes more rapid as $\Gamma_d^0$ and $\Gamma_n^0$ approach equality. Similarly $\mu_n$ has a rapid change, but in the opposite sense to $\mu_d$. The width of the dip in $\tau$ is determined more by the value of $\Gamma_d^0+\Gamma_n^0$ than by that of $\Gamma_d^0-\Gamma_n^0$. As a schematic illustration, the energy dependence of $\mu$ and $\tau$ in a one-level, two-channel case is given in Fig. 3 of Ref. [29], for a range of ratios of the partial widths. From the present one-level fit of the $\sigma_{dn}$ and $\sigma_T$ data, the predicted phase shifts are shown in Fig. 4.

The character of the real parts of the phase shifts, $\mu_d$ and $\mu_n$, whether they increase rapidly or decrease rapidly at the resonance energy, is determined by the relative size of the partial widths $\Gamma_d(E_r)$ and $\Gamma_n(E_r)$. Expressed in different terms, the character is determined by whether the scattering amplitudes $f_d$ and $f_n$, given by Eq. (4), when plotted on an Argand diagram, do or do not go round the point $i/2$, or equivalently whether $S_{dd}$ and $S_{nn}$ do or do not go round the origin. In the four-level fit of Hale *et al.* [8], $S_{nn}$ (shown in Fig. 3) does go round the origin, indicating a rapid increase of $\mu_n$ at the resonance and a rapid decrease of $\mu_d$. On the other hand, for the one-level fit (Table I), $S_{nn}$ does not go round the origin (while $S_{dd}$, which is also shown in Fig. 3, does), so that $\mu_n$ decreases rapidly at the resonance while $\mu_d$ increases, as shown in Fig. 4(a). This corresponds to $\Gamma_d(E_r)>\Gamma_n(E_r)$, which was also favored by Jarmie *et al.* [3], Hoop and Barschall [12], Balashko [17], and Kunz [30], who compared $^3$H$(d,n)^4$He and $^3$He$(d,p)^4$He cross sections.

(5) The real part of the $^3$He$+d$ elastic scattering $s$-wave phase shift is observed to rise smoothly through the $\frac{3}{2}^+$ resonance at a c.m. energy of about 270 keV [14]. Consistent with this, the $^4$He$+p$ $d_{3/2}$ phase shift is observed to decrease sharply at the resonance [31]. These indicate that $\Gamma(^3\text{He}+d,E_r)>\Gamma(^4\text{He}+p,E_r)$. One expects $\Gamma(^4\text{He}+p,E_r)\approx\Gamma_n(E_r)$ (for $^4$He$+n$), since the reduced widths should be about the same (from charge symmetry) and the

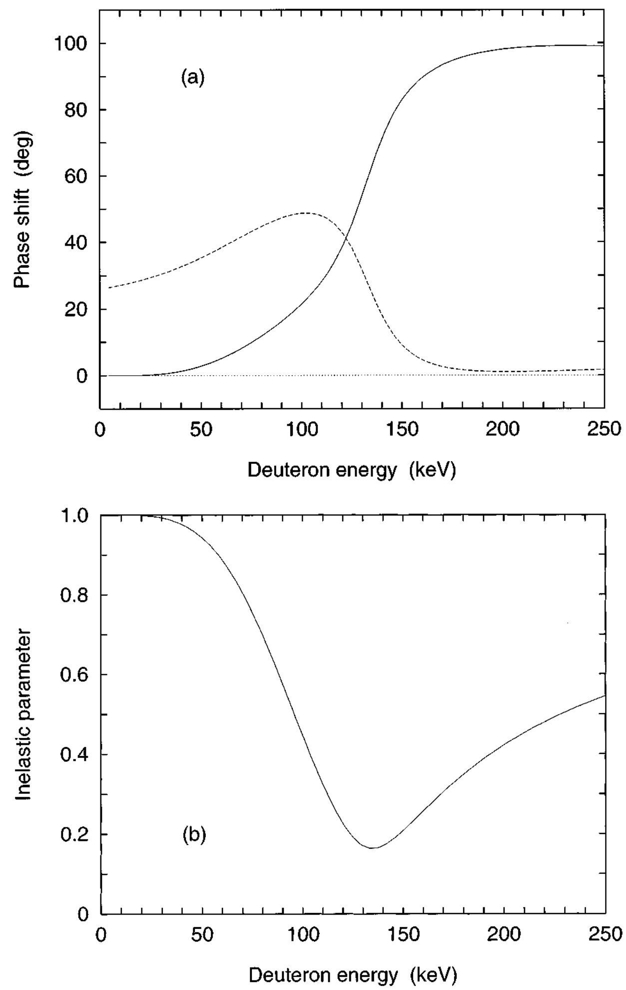


FIG. 4. (a) Predictions from the one-level fit to $\sigma_{dn}$ and $\sigma_T$ data, for the real parts of the $^3$H$+d$ $s$-wave phase shift $\mu_d$ (solid curve) and the $^4$He$+n$ $d_{3/2}$-wave phase shift $\mu_n$ (dashed curve), plotted as functions of deuteron lab energy $E_d$. (b) The corresponding inelastic parameter $\tau$.

penetration factors are about the same, because of the large channel energies involved. In comparing $\Gamma(^3\text{He}+d,E_r)$ with $\Gamma_d(E_r)$ (for $^3$H$+d$), the reduced widths should be about equal, but the calculated penetration factors differ, with a ratio about 2.5:1; the effect of the larger Coulomb barrier is outweighed by the higher resonance energy. Thus, even if there were some ambiguity in the relative sizes of $\Gamma_d(E_r)$ and $\Gamma_n(E_r)$ for the $^5$He level, there is no uncertainty in the expectation for the $^5$Li case.

More quantitatively, we calculate the $^3$He$+d$ and $^4$He$+p$ phase shifts, assuming the one-level approximation with the values of the reduced widths as in Table I. The value of $E_1$ is adjusted to best fit $^3$He$(d,p)^4$He data. Figure 5 shows results from two [32,33] of the several measurements (see Ref. [31]) that find varying positions and heights for the peak in the $^3$He$(d,p)^4$He cross section, and our calculated cross section using $E_1=E_r=0.450$ MeV. The corresponding phase shifts are given in Fig. 6, in reasonable agreement with the measured values [14,31].

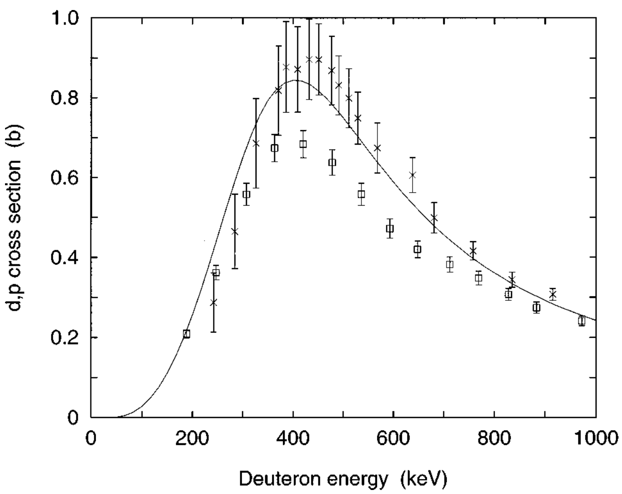


FIG. 5. Cross section for the $^3$He$(d,p)^4$He reaction as a function of deuteron lab energy. The experimental data are from Bonner *et al.* [32] (squares) and Yarnell *et al.* [33] (crosses). The calculated curve is the one-level fit with only the value of $E_r$ adjusted.

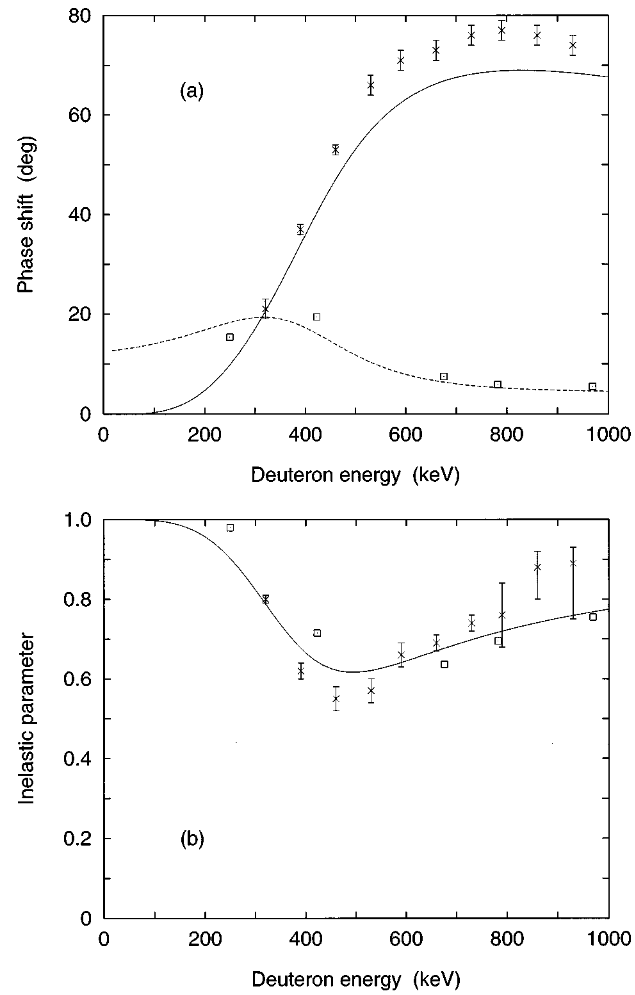


FIG. 6. (a) Real parts of the $^3$He$+d$ $s$-wave phase shift (crosses and solid curve) and the $^4$He$+p$ $d_{3/2}$-wave phase shift (squares and dashed curve), as functions of deuteron lab energy. The experimental points are from Jenny *et al.* [14] and Plattner *et al.* [31], respectively. The curves are predictions from the one-level fit, with $E_r$ adjusted to fit the $^3$He$(d,p)^4$He data (Fig. 5), and the background proton phase shift taken as a linear function of energy fitting the extreme values in Fig. 1 of Ref. [31]. (b) The corresponding inelastic parameter.

### C. Discussion

In the $R$-matrix description of the properties of the $\frac{3}{2}^+$ level of $^5$He (Sec. II B), the critical factors are the approximate equality at resonance of the partial widths in the deuteron and neutron channels, $\Gamma_d(E_r)$ and $\Gamma_n(E_r)$, and the sensitivity of some quantities to the sign of their difference. These factors account directly for the character of the state, the large value of the cross section $\sigma_{dn}$ at resonance, the rapid changes in the phase shifts $\mu_d$ and $\mu_n$ as one passes through the resonance, and also the behavior of the corresponding phase shifts at the $\frac{3}{2}^+$ resonance in $^5$Li.

In the description in terms of the poles of the $S$ matrix (Sec. II A), the analogous factors are the proximity of the shadow pole to the real axis, and the sensitivity to the Riemann surface on which the shadow pole lies. The correspondence between the vanishing of $\Gamma$ for the shadow pole and the vanishing of the inelastic parameter at resonance [which is equivalent from Eq. (21) to the exact equality of $\Gamma_d(E_r)$ and $\Gamma_n(E_r)$] has been pointed out previously [6]. It is apparent that, when $\Gamma_d(E_r)$ and $\Gamma_n(E_r)$ are about equal, or equivalently, when $\Gamma$ for the shadow pole is small, slight changes in the parameter values can change the characters of the phase shifts $\mu_d$ and $\mu_n$, from a rapid increase at resonance to a rapid decrease, or vice versa. Hale *et al.* [8] have defined partial widths at an $S$-matrix pole by $\Gamma_c=|\rho_{0c}|^2$, where the residue of $S$ at the pole is $i\rho_0\rho_0^T$, but these partial widths do not satisfy $\Sigma_c\Gamma_c=\Gamma$, where $E_r-i\Gamma/2$ is the complex energy of the pole. While $\Sigma_c\Gamma_c\approx\Gamma$ for the conventional pole, this is far from the case for the shadow pole [8,13]. The relationship, if any, between the $\Gamma_c$ and $\Gamma$ for the shadow pole has not been made clear in Refs. [8,13].

Eden and Taylor [9] have considered a simple one-level, two-channel resonance model, in which each channel is an $s$-wave neutral channel; in this model the properties of the $S$-matrix poles can be studied relatively easily. With the channels labeled 1 and 2, and the complex residues of $S_{cc'}$ at the conventional and shadow pole labeled $r^p_{cc'}$ (with $p=C$ and $S$, respectively), one finds $\Gamma^p\approx|r^p_{11}+r^p_{22}|$ for both poles, but particularly for the shadow pole and for $\Gamma^S$ small. In fact, one can show that $|r^S_{11}+r^S_{22}|/\Gamma^S\to 1$ as $\Gamma^S\to 0$. For the conventional pole, the arguments of $r^C_{11}$ and $r^C_{22}$ tend to be similar so that $|r^C_{11}+r^C_{22}|\approx|r^C_{11}|+|r^C_{22}|$; with Hale *et al.*'s definition of a partial width, one then finds a relation between the partial widths and $\Gamma^C$ similar to that found by Hale *et al.* [8]. For the shadow pole, the arguments of $r^S_{11}$ and $r^S_{22}$ differ by about 180° so that $|r^S_{11}+r^S_{22}|\approx||r^S_{11}|-|r^S_{22}||$; this gives

$$\Gamma^S\approx|\Gamma^S_1-\Gamma^S_2|. \tag{24}$$

Actually the relative argument of the residues $r^p_{11}$ and $r^p_{22}$ at either pole (conventional or shadow) is just the relative argument of the wave numbers $k_1$ and $k_2$ at the pole. For the shadow pole, as $\Gamma^S\to 0$, the relative argument of $r^S_{11}$ and $r^S_{22}$ tends to 180° exactly, so that Eq. (24) tends to an equality. Although the numerical values of the partial widths given by

Hale *et al.* [8] in their Table III do not satisfy a relation like (24), because of the surprisingly large value of $\Gamma_d^S$, it is tempting to suggest that $\Gamma^S$ for the shadow pole is approximately the difference of the $R$-matrix (observed) partial widths, and that it determines the energy interval over which the phase shifts $\mu_d$ and $\mu_n$ change rapidly [see Fig. 1(a) and Table I in Ref. [13]].

### D. Conclusion

It seems that the observed properties of the $\frac{3}{2}^+$ level in $^5$He and its analog in $^5$Li can be understood as easily in terms of the $R$-matrix parameters themselves as from the positions and residues of the complex-energy poles of the $S$ matrix.


[1] F. Ajzenberg-Selove, Nucl. Phys. **A490**, 1 (1988).

[2] G. M. Hale and D. C. Dodder, in *Nuclear Cross Sections for Technology*, NBS Spec. Publ. No. 594, edited by J. L. Fowler, C. H. Johnson, and C. D. Bowman (National Bureau of Standards, Washington, D.C., 1980), p. 650.

[3] N. Jarmie, R. E. Brown, and R. A. Hardekopf, Phys. Rev. C **29**, 2031 (1984).

[4] R. E. Brown, N. Jarmie, and G. M. Hale, Phys. Rev. C **35**, 1999 (1987).

[5] G. M. Hale, in *Neutron Standards and Applications, Gaithersburg, 1977*, NBS Spec. Publ. No 493, edited by C. D. Bowman, A. D. Carlson, H. O. Liskien, and L. Stewart (National Bureau of Standards, Washington, D.C., 1977), p. 30.

[6] B. C. Pearce and B. F. Gibson, Phys. Rev. C **40**, 902 (1989).

[7] A. Csoto and G. M. Hale, Phys. Rev. C **55**, 536 (1997).

[8] G. M. Hale, R. E. Brown, and N. Jarmie, Phys. Rev. Lett. **59**, 763 (1987); **59**, 2819 (1987).

[9] R. J. Eden and J. R. Taylor, Phys. Rev. **133**, B1575 (1964).

[10] H. V. Argo, R. F. Taschek, H. M. Agnew, A. Hemmendinger, and W. T. Leland, Phys. Rev. **87**, 612 (1952).

[11] B. Haesner, W. Heeringa, H. O. Klages, H. Dobiasch, G. Schmalz, P. Schwarz, J. Wilczynski, B. Zeitnitz, and F. Käppeler, Phys. Rev. C **28**, 995 (1983).

[12] B. Hoop and H. H. Barschall, Nucl. Phys. **83**, 65 (1966).

[13] A. Csoto, R. G. Lovas, and A. T. Kruppa, Phys. Rev. Lett. **70**, 1389 (1993).

[14] B. Jenny, W. Grüebler, P. A. Schmelzbach, V. König, and H. R. Bürgi, Nucl. Phys. **A337**, 77 (1980).

[15] A. M. Lane and R. G. Thomas, Rev. Mod. Phys. **30**, 257 (1958).

[16] L. N. Bogdanova, G. M. Hale, and V. E. Markushin, Phys. Rev. C **44**, 1289 (1991).

[17] Y. G. Balashko, in *Studies of Nuclear Reactions*, Proceedings of the P. N. Lebedev Physics Institute, Academy of Sciences of the USSR, Vol. 33, edited by D. V. Skobel'tsyn (Consultants Bureau, New York, 1966), p. 51.

[18] R. G. Thomas, Phys. Rev. **81**, 148 (1951).

[19] M. H. Macfarlane and J. B. French, Rev. Mod. Phys. **32**, 567 (1960).

[20] F. Ajzenberg-Selove and T. Lauritsen, Nucl. Phys. **11**, 1 (1959).

[21] F. C. Barker and C. L. Woods, Aust. J. Phys. **38**, 563 (1985).

[22] F. C. Barker, Proc. Phys. Soc. London **84**, 681 (1964).

[23] J. E. Bond and F. W. K. Firk, Nucl. Phys. **A287**, 317 (1977).

[24] R. K. Adair, Phys. Rev. **86**, 155 (1952).

[25] D. C. Dodder and J. L. Gammel, Phys. Rev. **88**, 520 (1952).

[26] C. L. Woods, F. C. Barker, W. N. Catford, L. K. Fifield, and N. A. Orr, Aust. J. Phys. **41**, 525 (1988).

[27] J. P. Conner, T. W. Bonner, and J. R. Smith, Phys. Rev. **88**, 468 (1952).

[28] R. E. Shamu and J. G. Jenkin, Phys. Rev. **135**, B99 (1964).

[29] J. M. Morris, G. W. Kerr, and T. R. Ophel, Nucl. Phys. **A112**, 97 (1968).

[30] W. E. Kunz, Phys. Rev. **97**, 456 (1955).

[31] G. R. Plattner, A. D. Bacher, and H. E. Conzett, Phys. Rev. C **5**, 1158 (1972).

[32] T. W. Bonner, J. P. Conner, and A. B. Lillie, Phys. Rev. **88**, 473 (1952).

[33] J. L. Yarnell, R. H. Lovberg, and W. R. Stratton, Phys. Rev. **90**, 292 (1953).